The current issue and full text archive of this journal is available at
www.emeraldinsight.com/0332-1649.htm



# Calculation of the flux distribution of three phase five limb power transformers considering nonlinear material properties

Björn Riemer, Enno Lange and Kay Hameyer
*Institute of Electrical Machines, RWTH Aachen University, Aachen, Germany*

## Abstract

**Purpose** – Depending on the load the flux-density distribution inside power transformers core shows significant local variations due to stray fluxes which enter the transformer core. As saturation of the core has to be avoided the flux-density distribution has to be determined early in the design stage of the transformer. This paper seeks to address these issues.

**Design/methodology/approach** – To determine the load dependent flux-density distribution the operating point of the transformer is calculated considering linear and non-linear material properties. The operating point is determined using a linearised lumped parameter model of the transformer under various load conditions. Considering non-linear material properties the inductance matrix depends on the operating point and will be extracted by means of the FEM whenever the magnetic energy within the transformer changes notably.

**Findings** – This paper presents a numerical stable approach to calculate the operating point of a transformer by using the magnetic flux linkage as state variable for the coupled field problem.

**Research limitations/implications** – The proposed approach uses a fixed time-step to update the lumped parameters by means of the FEM. This results in long simulation times. In further research it is planned to implement an adaptive time-step method based on the change of the magnetic energy.

**Originality/value** – A numerical stable approach to calculate the operating point of a transformer by using the magnetic flux linkage as state variable for the coupled field problem is proposed. The methodology is applied to a 2D model of a three-phase transformer. However, it also can be applied to 3D FE models. Based on the calculated operating point, the flux-density distribution can be determined and several post-processing methods can be executed (e.g. determination of core losses, . . .).

**Keywords** Field circuit coupling, Flux-density distribution, Load dependent stray fluxes, Transformer core saturation, Phase shifting transformer, Transformers, Flux density, Fluxes

**Paper type** Research paper

## 1. Introduction

The deregulation of the energy market causes fundamental changes on the requirements of the network configuration. The power flow in international interconnected systems, as well as the increased supply of renewable energy sources leads to additional stresses on individual network areas. To avoid congestions power flow controllers like phase-shifting transformers (PST) are used to control the power flow inside the grid. PSTs control the power flow over a transmission line by impressing a controllable quadrature voltage between their connection points. Based on the rated power and the requirements of the control, different principles of PSTs as given in Kramer and

The authors gratefully acknowledge the technical and financial support of the ABB AG – Bad Honnef.

COMPEL: The International Journal for Computation and Mathematics in Electrical and Electronic Engineering
Vol. 32 No. 4, 2013
pp. 1230-1243

0332-1649
DOI 10.1108/03321641311317059

Ruff (1998) can be applied. An equivalent circuit diagram (ECD) of an indirect symmetrical PST and its phasor diagram is shown in Figure 1. The quadrature voltage is controlled by tap windings of the exciter transformer.

In PSTs of the two core design as shown in Figure 1 especially the stray flux of the exciter transformer, caused by load currents, is predominantly in phase or in phase opposition to the exciting flux of the core, similar to the conditions in regular transformers under capacitive or inductive load. Due to the superposition of exciting and stray flux significant local variations of the core fluxes may occur especially in the yoke. Generally the yoke cross-section of a five limb transformer is approximately 60 per cent of the main limb cross-section. For economical reasons a decrease of the yoke cross-section is desired. Since saturation of the core has to be avoided definitely possible load-dependent local flux variations especially under capacitive load have to be considered already in the design stage.

This paper describes an approach to investigate the flux distribution inside the transformer core using a linearised lumped parameter model of the transformer under various load conditions. The model is based on a lumped inductance matrix representation, whose values are extracted by means of the finite element method (FEM) whenever the magnetic energy within the transformer changes notably.

First the theoretical framework of the proposed approach is described. Then the approach is applied to a three phase five limb exciter transformer of a PST considering linear and non-linear material properties. Finally results of the flux-density computation using linear and non-linear material properties for a 2D FE model of the transformer are compared.

## 2. Theoretical framework

This section describes the theoretical framework of the electromagnetic calculations. It is described how to determine the operating point of a transformer considering linear and non-linear material properties and furthermore how the flux distribution inside the transformer core is calculated. The transformer is represented by linearised lumped parameter and therefore by the differential equations:

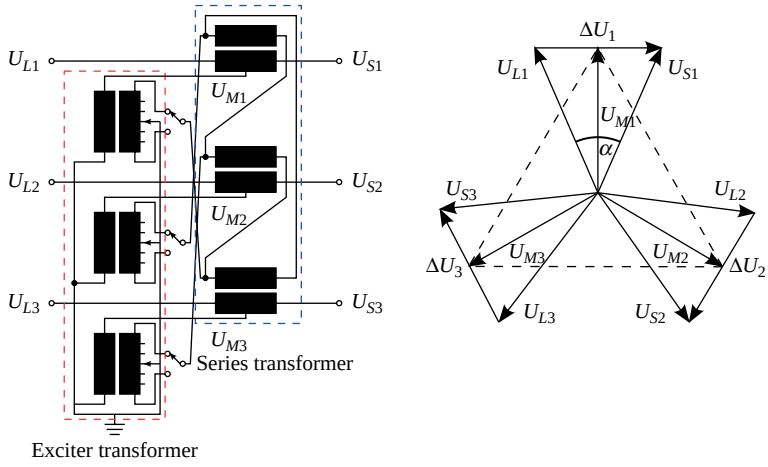


**Figure 1.**
ECD and phasor diagram of an indirect symmetrical PST

$$\mathbf{u}(t) = \mathbf{R} \cdot \mathbf{i}(t) + \frac{d}{dt}\boldsymbol{\Psi}(\mathbf{i}, t), \tag{1}$$

with the phase voltages **u**, the winding resistance matrix **R**, the phase currents **i** and the flux linkage matrix $\boldsymbol{\Psi}$. The inductance matrix is extracted systematically using a method which is already described in Lange *et al.* (2009) and Henrotte *et al.* (2007). Based on the parameter extraction Subsection 2.2 describes a model for the linear and non-linear calculation of the operating point. Subsection 2.3 describes the calculation of the magnetic flux distribution inside the transformer core.

*2.1 Determination of the inductance matrix*

The lumped parameters that represent a transformer are the winding resistances and inductances. Any capacitive effects are neglected. Considering a simplified model for a transformer winding as hollow cylinder the winding resistances can be determined analytically by:

$$R_{wind} = \frac{\pi \cdot d_m}{\sigma \cdot A \cdot k_{co}}, \tag{2}$$

with the mean winding diameter $d_m$, the specific electrical conductivity $\sigma$, the coil cross-section area $A$ and the copper fill-factor $k_{co}$.

The inductances are extracted systematically from a FE model of the transformer as described already in Lange *et al.* (2009). The presented approach can be applied to 2D and 3D FE models. It consists in exploiting the FE Jacobian matrix of the magnetic system, which represents the first order linearisation of the non-linear field equations around the operating point at time $t$. A mapping between the field state variable (the magnetic vector potential **a**) and the circuit state variables (the phase fluxes $\varphi_r$) is obtained on basis of energy considerations.

The energy balance of a magneto-dynamic system expressed in field quantities stating a power balance yields:

$$\dot{E}_M - \dot{W}_m = \int_\Omega \mathbf{j} \cdot \mathcal{L}_\mathrm{v}\mathbf{a}, \tag{3}$$

and, respectively, in terms of circuit quantities:

$$\dot{E}_M - \dot{W}_m = \sum_r i_r \dot{\varphi}_r. \tag{4}$$

$\dot{E}_M$ is the time derivative of the magnetic energy. $\dot{W}_m$ is the power delivered by magnetic forces, which is zero neglecting magnetostriction, and $\mathcal{L}_\mathrm{v}\mathbf{a}$ is the material derivative of **a**. Absence of motion or deformation of the domain $\Omega$ yields $\mathcal{L}_\mathrm{v} = (\mathrm{d}/\mathrm{d}t)$. $\dot{\varphi}_r$ is time derivative of the flux through the coil winding of phase $r$. The current density **j** in stranded conductors can be written as:

$$\mathbf{j} = \sum_r i_r \mathbf{w}_r, \tag{5}$$

where $\mathbf{w}_r$ are the shape functions of the phase currents $i_r$. Using equations (3) and (4) and substituting (5) yields:

$$\dot{\varphi}_r = \int_\Omega \mathbf{w}_r \cdot \mathcal{L}_v \mathbf{a} d\Omega. \tag{6}$$

In the absence of eddy currents the current shape functions $\mathbf{w}_r$ are independent of time. Thus, the mapping between $\mathbf{a}$ and $\varphi_r$ is:

$$\varphi_r = \int_\Omega \mathbf{w}_r \cdot \mathbf{a} d\Omega. \tag{7}$$

In a mesh, this mapping between $\mathbf{a}$ and $\varphi_r$ can be expressed by the vector:

$$W_{ri} = \int_\Omega \mathbf{w}_r \cdot \alpha_i d\Omega \quad \varphi_r = W_{ri} a_i \tag{8}$$

where $\alpha_i$ are the shape functions of the $\mathbf{a}$ field, and $a_i$ the corresponding coefficients.

The non-linear FE magneto-static equation system describing the transformer under applied load currents is:

$$M_{ij}(\mathbf{a}) a_j = b_i \tag{9}$$

with:

$$b_i = \int_\Omega \mathbf{j} \cdot \alpha_i d\Omega = I_r \int_\Omega \mathbf{w_r} \cdot \alpha_i d\Omega = I_r W_{ir}. \tag{10}$$

Let $I_r^*$ be the currents at time $t$, and $b_i^* = I_r^* W_{ir}$ the corresponding right-hand sides. Solving equation (9) with $b_i \equiv b_i^*$ gives $a_j^*$ and a first order linearisation around this particular solution writes:

$$M_{ij}\left(a_j^* + \delta a_j\right) = M_{ij} a_j^* + J_{ij} \delta a_j = b_i^* + \delta b_i \tag{11}$$

with the Jacobian Matrix $J_{ij} \equiv (\partial_{a_j} M_{ik}) a_k^*$. Since $M_{ij} a_j^* = b_i^*$, one has:

$$J_{ij} \delta a_j = \delta b_i. \tag{12}$$

One can now repeatedly solve equation (12) with the right-hand sides $\delta b_i = \delta I_r W_{ir}$ obtained by perturbating one after the other $m$ phase currents $I_r$ and obtain $m$ solution vectors for $\delta a_j$. Since equation (12) is linear, the magnitude of the perturbations $\delta I_r$ is arbitrary. One can so define by inspection the partial inductance matrix $L_{rs}^\partial$ of the transformer seen from the terminals as:

$$\begin{aligned} \delta\varphi_r &= W_{rj} \delta a_j \\ &= W_{rj} J_{ji}^{-1} W_{is} \delta I_s \\ &\equiv L_{rs}^\partial \delta I_s \end{aligned} \tag{13}$$

with:

$$L_{rs}^\partial = W_{rj} J_{ji}^{-1} W_{is}. \tag{14}$$

Similarly one can identify the secant inductance matrix $L_{rs}$ and by solving equation (9) repeatedly with linearly independent phase currents $I_r$ to obtain:

$$\begin{aligned}\varphi_r &= W_{rj}\delta a_j \\ &= W_{rj}M_{ji}^{-1}W_{is}I_s \\ &\equiv L_{rs}I_s\end{aligned} \tag{15}$$

with:

$$L_{rs} = W_{rj}M_{ji}^{-1}W_{is}. \tag{16}$$

*2.2 Calculation of the operating point*

*2.2.1 Linear material properties*. An arbitrary operating point of the transformer can be determined solving equation (1). As described in Section 1 the inductance matrix $\mathbf{L}$ is extracted by means of the FEM. Considering linear material properties the secant inductance matrix $\mathbf{L}$ is constant, the time derivative of the flux linkage matrix is given by:

$$\frac{d}{dt}\mathbf{\Psi}(\mathbf{i}, t) = \mathbf{L}\cdot\frac{d}{dt}\mathbf{i}(t). \tag{17}$$

For the inductance matrix it is assumed $L_{i,j} = L_{j,i}$. To avoid numerical inaccuracies the extracted inductance matrix is balanced by:

$$\mathbf{L} = \frac{\mathbf{L}_{FE} + \mathbf{L}_{FE}^{T}}{2}. \tag{18}$$

This symmetrisation does not include any geometrical symmetries and does not affect the results.

Considering a steady state operation the time derivative can be expressed by a time harmonic-approach:

$$\frac{d}{dt} = j\omega. \tag{19}$$

The primary winding of the transformer is excited by a voltage. The secondary winding is loaded with an arbitrary impedance, as shown in Figure 2.

The voltage $\underline{\mathbf{u}}_1$ represents a vector including the primary phase-shifted phase voltages of the three phase system. Consequently, the inductance $\mathbf{L}_{11}$ and $\mathbf{L}_{22}$ are matrices including all self and mutual inductances of the primary, respectively, the secondary three phase winding system. The coupling elements $\mathbf{L}_{12}$ and $\mathbf{L}_{21}$ are matrices that include all mutual inductances of the primary to the secondary winding system and vice versa. The resistances $\mathbf{R}_{1,2}$ and the load impedance $\mathbf{Z}_{Load}$ are diagonal matrices.

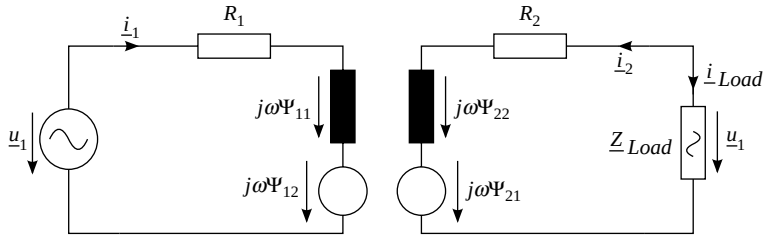


**Figure 2.**
Electrical ECD of the transformer

Applying equations (17), (19) and $\underline{\mathbf{u}}_2 = \underline{\mathbf{i}}_{Load} \cdot \underline{\mathbf{Z}}_{Load} = -\underline{\mathbf{i}}_2 \cdot \underline{\mathbf{Z}}_{Load}$ to equation (1) the unknown phase currents can be calculated by:

$$\begin{pmatrix} \underline{\mathbf{i}}_1 \\ \underline{\mathbf{i}}_2 \end{pmatrix} = \left[ \begin{pmatrix} \mathbf{R}_1 & 0 \\ 0 & \mathbf{R}_2 \end{pmatrix} + j\omega \begin{pmatrix} \mathbf{L}_{11} & \mathbf{L}_{12} \\ \mathbf{L}_{21} & \mathbf{L}_{22} \end{pmatrix} + \begin{pmatrix} 0 & 0 \\ 0 & \underline{\mathbf{Z}}_{\mathrm{Load}} \end{pmatrix} \right]^{-1} \cdot \begin{pmatrix} \underline{\mathbf{u}}_1 \\ 0 \end{pmatrix}. \quad (20)$$

Once the inductance matrix is determined each arbitrary operating point can be calculated with negligible computational cost.

*2.2.2 Nonlinear material properties*. Considering non-linear material properties the inductance matrix depends on the operating point, i.e. the load, and thus on the saturation state of the transformer core. This yields a coupled simulation problem. The differential equation system of the electric circuit equation (1) can be solved by using a lumped parameter model representing the field problem. The field problem is solved by a computationally expensive FE calculation. The extracted lumped parameters from the FEM are updated with an arbitrary update rate of $\Delta T_{FE}$ which is lower than the circuit problem time step. Figure 3 shows a flowchart of the weak coupled simulation. Initially, the tangent inductance matrix ($L_{rk}^{\partial k}$) is extracted by a static FE analysis. The circuit problem is solved for a time interval up to the update rate of the field problem. At the update point the excitation currents which are calculated by the circuit equations are set and an updated tangent inductance matrix is extracted and the circuit problem is solved for the next time interval. The coupled simulation ends if a defined end time $t_{end}$ is reached.

Taking the phase current as state variable for the coupled problem, the circuit equation system (1) for the no load case yields:

$$\frac{d}{dt}\mathbf{i} = \mathbf{L}^{\partial -1}[\mathbf{u} - \mathbf{R}\mathbf{i}]. \quad (21)$$

For this model there is no feedback between flux linkages calculated by the circuit problem ($\Psi = L^{\partial} i$) and the field problem ($\Psi = \int_{\Omega} \mathbf{w}_r \cdot \mathbf{a}$, with the current shape function $\mathbf{w}_r$, the coildomain $\Omega$ and the magnetic vector potential $\mathbf{a}$). The linearisation of the tangent inductance matrix leads to an error which propagates in time. Due to the missing feedback the simulation will diverge as it is shown in Figure 4. The figure

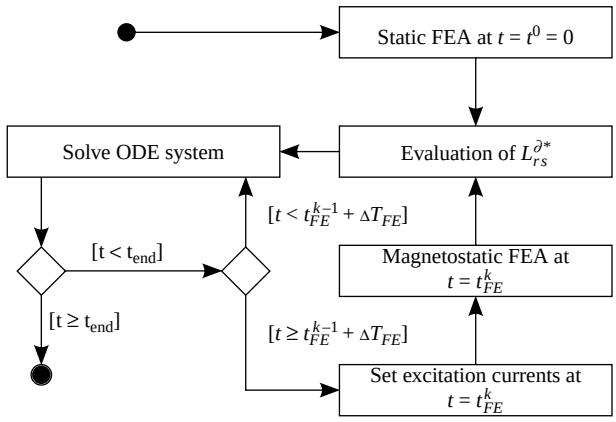


**Figure 3.**
Flowchart of the coupled simulation

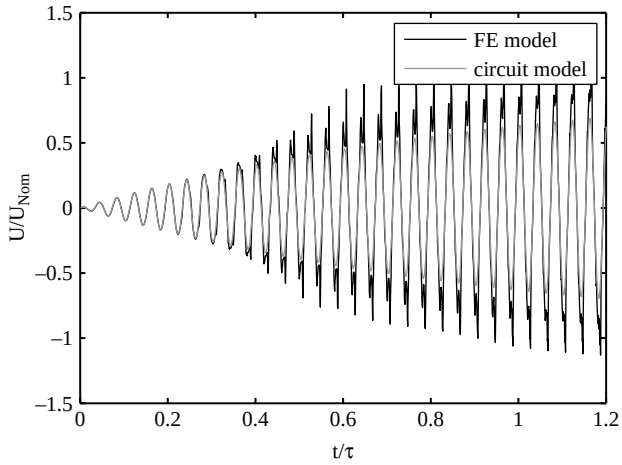


**Figure 4.**
Comparison induced voltage of one phase taking the phase current as state variable

depicts the induced voltage in one phase of a three phase transformer at starting operation. To decrease the transient phenomenon the magnitude of the exciting voltage is increased with an exponential function with the time constant $\tau$. At $t \approx 0.3\tau$ the simulation diverges. The flux linkage and consequentially the induced voltage calculated by the FE model exceeds the induced voltage calculated by the circuit problem, because of erroneously impressed currents.

A stable behaviour for the coupled problem can be achieved by taking the flux linkage as state variable. At each extraction step the tangent inductance matrix and the flux, respectively, the flux linkage $\Psi|_{t_{FE}^k}$ is extracted from the magneto static FE analysis at the time step $t_{FE}^k$. The circuit equation yields:

$$\int_{-\infty}^{t} (\mathbf{u} - \mathbf{R}\mathbf{i})dt = \boldsymbol{\Psi}\Big|_{t_{FE}^k} + \frac{\partial \boldsymbol{\Psi}}{\partial \mathbf{i}}\Big|_{t_{FE}^k} \left(\mathbf{i} - \mathbf{i}|_{t_{FE}^k}\right), \tag{22}$$

and consequently:

$$\mathbf{i}(t) = \left(\frac{\partial \boldsymbol{\Psi}}{\partial \mathbf{i}}\right)^{-1}\Big|_{t_{FE}^k} \left(\int_{-\infty}^{t} (\mathbf{u} - \mathbf{R}\mathbf{i})dt - \boldsymbol{\Psi}|_{t_{FE}^k}\right) + \mathbf{i}\Big|_{t_{FE}^k}. \tag{23}$$

The change in the current is calculated on basis of the flux linkages of the circuit equation and of the FE model. At each FE extraction point $t_{FE}^k$ the deviation of the flux linkage from the circuit problem and the FE problem is reset. Thus, discontinuities in the current characteristic are possible. Figure 5 shows the flux linkage and the current in one phase of the transformer. The discontinuities at the FE extraction points can be used as an error indicator to control the step width of the FE extraction points.

According to the calculation of the operating point considering linear material properties the load in equation (23) is considered by its differential equation, e.g. $\mathbf{u} = (1/C_{Load}) \int \mathbf{i}dt$ for the capacitive, respectively, $\mathbf{u} = L_{Load} d_t \mathbf{i}$ for the inductive load.

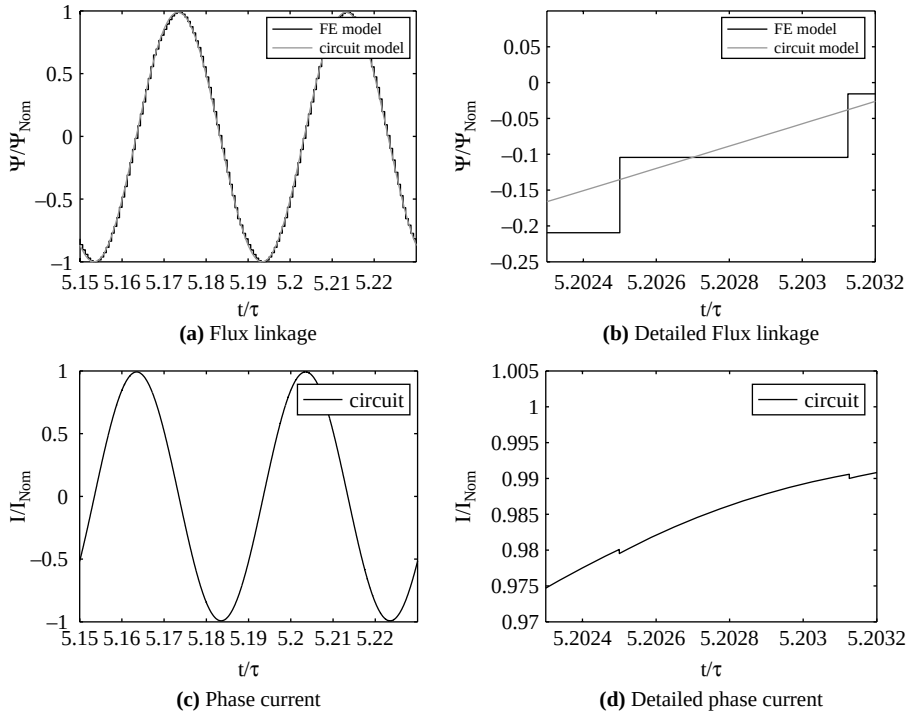


**(a)** Flux linkage

**(b)** Detailed Flux linkage

**(c)** Phase current

**(d)** Detailed phase current

**Figure 5.**
Flux linkage and current considering flux as state variable

*2.3 Determination of the flux-density distribution*

The flux is determined by the circulation of the magnetic vector potential over a closed contour $C$:

$$\varphi = \oint_C \mathbf{a}\mathrm{d}C. \tag{24}$$

For 2D FEA equation (24) simplifies to:

$$\varphi_i = (a(P_{i,1}) - a(P_{i,2})) \cdot d \tag{25}$$

with the depth of the 2D model $d$ and the vector potential solution at two arbitrary points $a(P_{i,1})$ and $a(P_{i,2})$ referring to Figure 6. In 3D the determination of the flux gets more complex as a closed contour on the transformer core has to be identified. The flux is calculated at $n$ points in different locations (side yoke, middle yoke, etc.) of the transformer core. Figure 6 shows exemplarily the $n$ calculation points at the side yoke of a five limb transformer.

For linear material properties the vector potential solution is available only for the unit excitation per coil $m$ of the winding configuration. Therefore, the flux inside the core is determined by:

$$\varphi|_{loc,i} = \sum_{r=1}^{m} \varphi_r|_{loc,i} i_r \quad \text{with} \quad \varphi_r|_{loc,i} = \oint_C \mathbf{a}_r \mathrm{d}C. \tag{26}$$

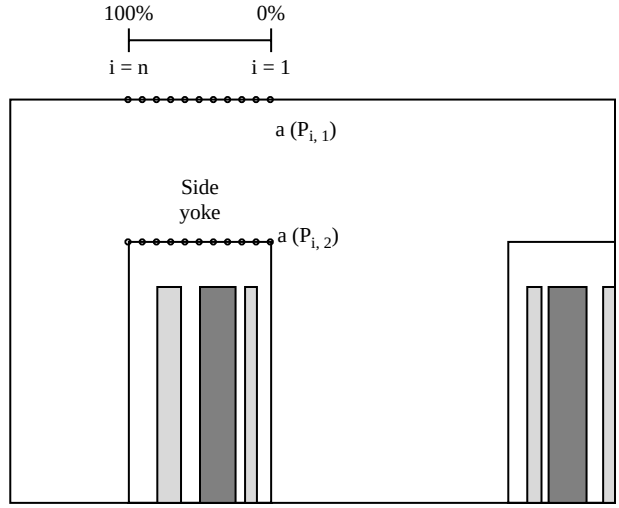


**Figure 6.**
Calculation points of the flux

The currents $i_r$ of the operating point are calculated by equation (20).

For a non-linear calculation as described in Section 2.2.2 the vector potential solution is available for each extraction point. Thus, equation (24) can directly be applied to the field solution of the operating point.

Towards the calculation of the flux distribution the mean flux-density distribution is calculated by:

$$\bar{B}|_{loc,i} = \frac{\varphi|_{loc,i}}{A_{cs,i}}, \tag{27}$$

where $A_{cs,i}$ is the flux penetrating cross-section area of the transformer core.

## 3. Calculation of the flux-density distribution

The proposed calculation method of the flux-density distribution is exemplarily applied to a five limb three phase transformer. In this paper a 2D FE model is used. However, as the proposed method is also valid for 3D FE-models it is possible to take into account the transformers tank, clamping plates, etc. The considered transformer has a double concentric winding configuration as it is used, e.g. in exciter transformers of PSTs in a power range of 100 MVA up to 2,000 MVA. The inner winding is connected in series with the outermost winding and is specified as primary winding. The middle winding is specified as secondary winding.

Figure 7 shows a schematic view of the five limb transformer. The flux-density distribution is calculated inside the yoke, the outer main limb and the side limb.

The operating point of the transformer is calculated under no-load condition and inductive, respectively, capacitive load conditions. For the non-linear calculation the B-H characteristic of grain-oriented electrical steel sheets with grade M-0H as shown in Figure 8 is considered. The linear calculations are performed assuming a relative permeability $\mu_r = 20{,}000$. The transformer is designed for a magnetic flux density inside the main limb of $B_{nom} = 1.52\text{T}$.

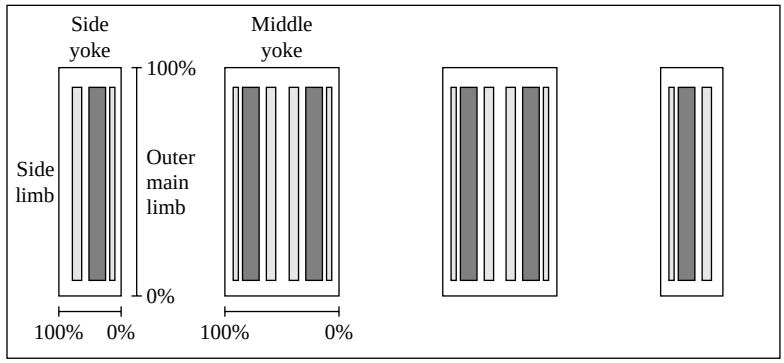


**Figure 7.**
Schematic view of a five limb transformer

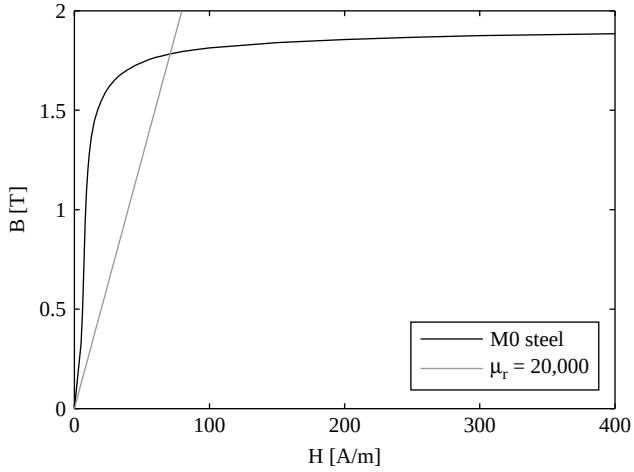


**Source:** Nippon Steel Corporation (2011)

**Figure 8.**
Non-linear B-H characteristic M-0H

First the no-load operation is calculated considering linear and non-linear material properties of the transformer core. The primary winding is connected to nominal voltage. The secondary winding is opened. The resulting no-load currents considering non-linear material properties are shown in Figure 9. Due to incipient saturation especially in the middle yoke the third and fifth harmonic occur with a magnitude of 9 per cent, respectively, 5 per cent.

The fundamental component of the flux-density distribution for the no-load case is shown in Figure 10. The mean flux-density distribution is calculated as described in Section 3 by means of equations (26) and (27). Inside the main limb the flux-density calculated considering linear and non-linear material is at the nominal flux-density. Due to the superposition of the fluxes of the three phases the flux-density increases at the middle yoke. Due to incipient saturation the flux-density of the linear calculation is higher compared to the non-linear calculation. Consequential the magnetic flux-density at the side yoke and side limb reduces for the linear case compared to the non-linear case.

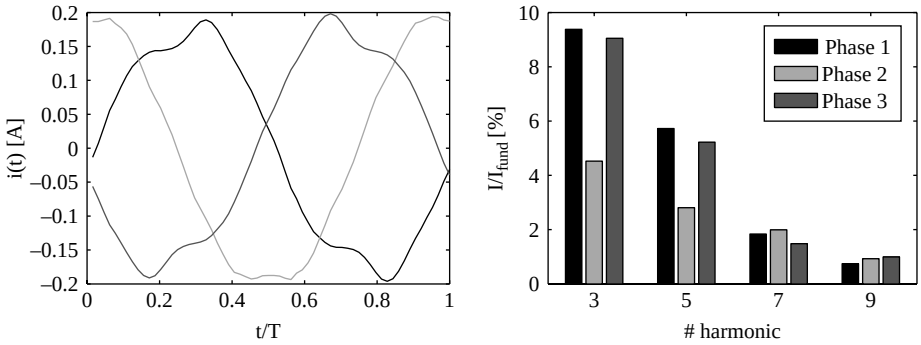


**(a)** Time series of the phase currents.

**(b)** Spectrum of the phase currents.

**Figure 9.**
No-load currents of the transformer considering nonlinear material properties

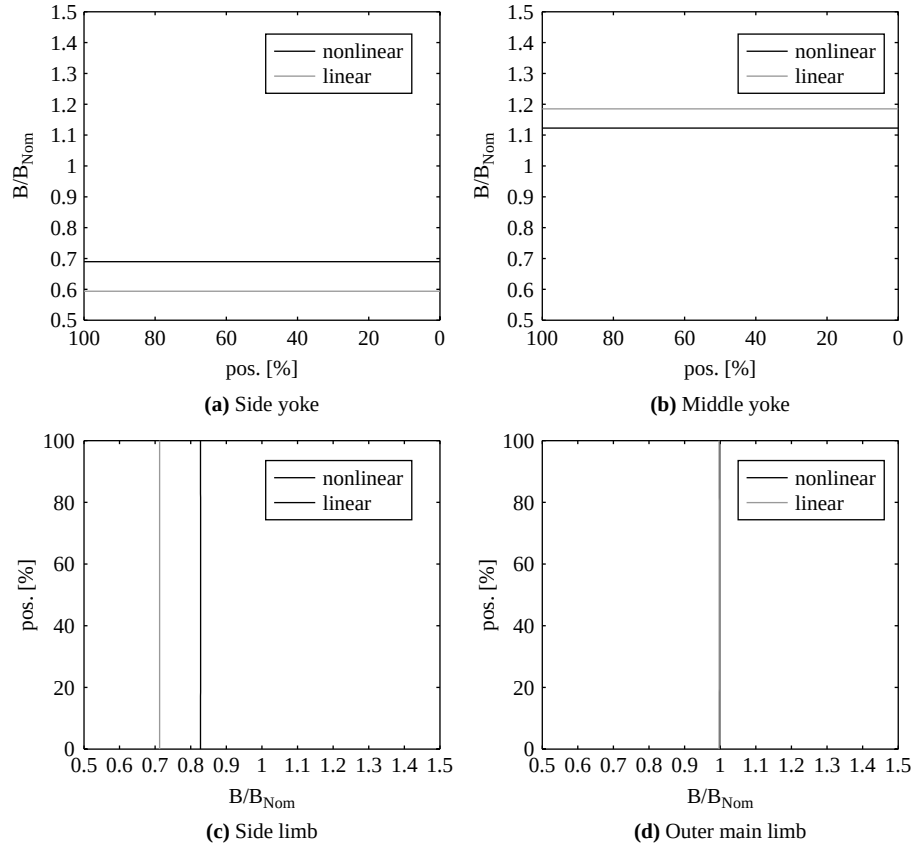


**(a)** Side yoke

**(b)** Middle yoke

**(c)** Side limb

**(d)** Outer main limb

**Figure 10.**
Magnetic flux density distribution: no-load operation

Applying a capacitive load to the secondary winding of the transformer leads to deviations of the flux-density distribution, due to stray fluxes which enters the core. The maximum flux-density appear at the side yoke. Figure 11 shows the flux-density distribution of the capacitive load case at nominal power referred to the no-load flux-density. The flux-density is increased about 2.1 per cent at the side yoke considering non-linear materials compared to the no-load operation.

Defining a reference stray flux $\Phi_{stray,ref} = u_k \cdot \Phi_{main}$ with the percent impedance $u_k = 2.58$ per cent, it can be stated that 81 per cent of the full stray flux enters the core at the side yoke. The percent impedance $u_k$ is determined by a short-circuit test using the linear equation system given in equation (20) with $\underline{\boldsymbol{Z}}_{Load} = 0$ and a nominal current flow in the primary winding. Inside the yoke the linear calculation offers a slightly higher fraction of stray flux entering the core compared to the non-linear results. Thus, the linear calculation can be used as a worst case approximation to evaluate the load-dependent stray fluxes entering the core for a certain geometry.

Applying an inductive load to the secondary winding of the transformer at nominal power leads to the flux-density distribution shown in Figure 12. For the inductive load operation the flux-density at the yoke is reduced, except the region between of two neighbouring phase windings at the middle yoke. There the flux-density is increased

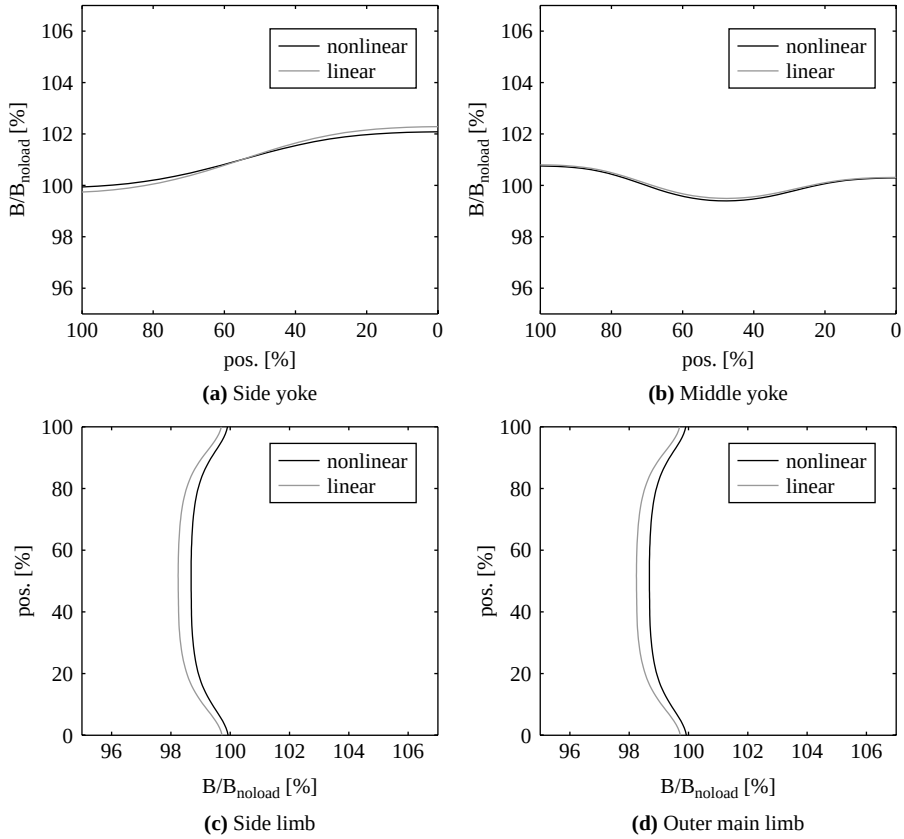


**Figure 11.**
Magnetic flux density-distribution: capacitive load conditions

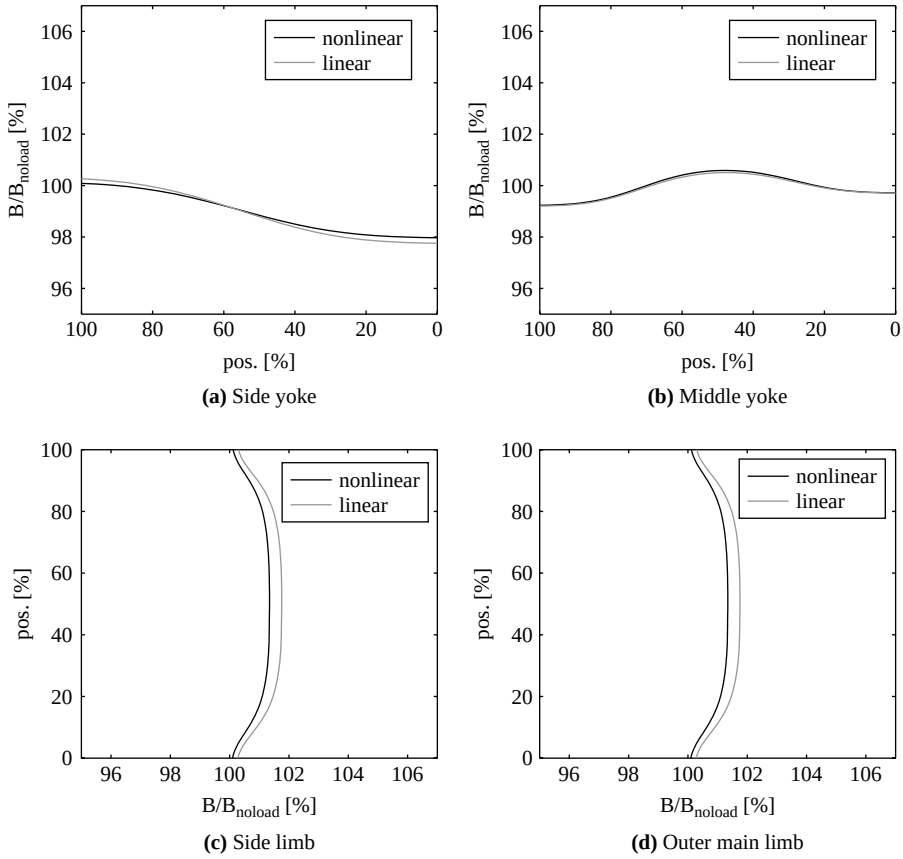


**Figure 12.**
Magnetic flux density distribution: inductive load conditions

about 0.6 per cent. At the main limb and the side limb the flux-density is slightly increased in opposition to the capacitive load case.

Comparing the flux-density distribution of the capacitive and the inductive load case, it can be stated that the capacitive load case is the more critical case for the design of the top yoke, if the primary winding is excited by a voltage.

## 4. Conclusions

This paper presents an approach for the calculation of the flux, respectively, flux-density distribution of power transformers considering non-linear material properties. The calculation is based on a linearised lumped parameter representation of the transformer. The resistances of the phase windings are calculated by a simplified analytical model as their influence on the results is insignificant. The inductance matrix is extracted by means of a FE model of the transformer. The proposed approach allows for the use of linear as well as non-linear material properties.

Considering linear material the inductance matrix do not depend on the operating point. Once the inductance matrix is extracted each operating point can be calculated with negligible computational cost.

For non-linear material properties the inductance matrix is extracted depending on the operating point of the transformer. It is shown that using the phase current as a state variable for the coupled field problem, the simulation will diverge, due to a linearisation error which propagates in time. By using the magnetic flux linkage as a state variable a numerical stable behaviour is obtained to accurately determine the transformers operating point.

The presented approach is applied to a five limb three phase power transformer. The flux-density distribution is calculated for the no-load as well as the inductive and capacitive load operation. Load dependent stray fluxes which enter the core are analysed for the different load cases. Considering the flux-density inside the yoke the capacitive load case is the more critical as the flux-density will increase about 2.1 per cent compared to the no-load case.

## References

Henrotte, F., van der Giet, M. and Hameyer, K. (2007), "Fluxes, inductances and their numerical computations", paper presented at 16th International Conference on the Computation of Electromagnetic Fields, COMPUMAG, Aachen, Germany.

Kramer, A. and Ruff, J. (1998), "Transformers for phase angle regulation considering the selection of on-load tap-changers", *IEEE Transactions on Power Delivery*, Vol. 13 No. 2, pp. 518-525.

Lange, E., Henrotte, F. and Hameyer, K. (2009), "An efficient field-circuit coupling based on a temporary linearization of FE electrical machine models", *IEEE Transactions on Magnetics*, Vol. 45 No. 3, pp. 1258-1261.

Nippon Steel Corporation (2011), *Orientcore·Orientcore HI-B®·Orientcore HI-B·LS®–Grain-Oriented Electrical Steel Sheets*, URL, available at: www.nsc.co.jp/en

**Corresponding author**
Björn Riemer can be contacted at: bjoern.riemer@iem.rwth-aachen.de